An Analytical Solution of the Lateral Current Spreading and Diffusion Problem in Narrow Oxide Stripe (GaAl)As/GaAs DH Lasers

G. LENGYEL, MEMBER, IEEE, PETER MEISSNER, ERWIN PATZAK, AND K.-H. ZSCHAUER

Abstract—**An exact solution is presented to the problem of lateral current spreading in the resistive layer of oxide stripe geometry DH lasers. The two-dimensional Laplace equation was solved by conformal mapping using the Schwarz-Christoffel transformation. The diffusion equation containing nonlinear recombination terms was solved numerically. Computed examples demonstrate that the customary one-dimensional treatment of the resistive layer or the assumption of constant current density under the stripe contact are not always justified, particularly for narrow stripe widths and low specific resistivities. This region of low values of the resistivity and stripe width, however, is of great practical interest in the design of oxide stripe lasers having high thermal stability and kink-free characteristics.**

I. Introduction

CONFINEMENT and guidance of the electromagnetic (EM) wave is a central problem in the design of efficient semiconductor lasers which are operated at room temperature in the CW mode. In GaAs-GaAlAs DH lasers, the EM wave is confined in the transverse direction by the finite step caused by the difference in the refractive indices of the two semiconducting materials [1]-[3]. No such firm guiding exists in the lateral direction in gain-guided stripe geometry DH lasers, where the spreading of the wave is prevented only by the optical gain [4], [5] produced by the large carrier densities in strongly pumped regions of the laser. Important laser operating parameters such as threshold current, width of the lateral modes, and stability of lateral modes are influenced by this lateral guidance and depend therefore on the lateral distribution of carriers and of the optical gain. The gain profile, on the other hand, is determined by the distribution of the pumping current which, below lasing threshold is affected by the following two physical processes:

1) lateral diffusion of carriers in the active region,

2) lateral current spreading in the resistive layer lying between the contact and the active region.

Above the lasing threshold, a third factor is added to the previous considerations, namely the stimulated recombination which is a function of the photon density profile of the EM wave.

The importance of lateral distributions was recognized early in the development of DH lasers [6]-[17]. All authors treat the series resistance effects approximately either by averaging over the thickness of the resistive layer (various sheet-resistance models), weighted averaging using simple functions [13], or correction factors [18] reducing the representation of the resistive layer to a single dimension. Others [8], [12], [13] employ assumed distributions of the pumping current density along the contact stripe or the p-n interface. With the exception of [16] all express the relationship for the potential across the junction in terms of current density rather than carrier density. None of the authors gives an exact solution for the current density distribution under the stripe contact.

A common shortcoming of these models is the essentially one-dimensional treatment of the resistive layer. As long as stripe width to resistive layer thickness ratios are relatively large, such approximations are permissible. It has become evident, however, over the last few years, that planar oxide stripe lasers having relatively large stripe width display kinks in their light-current characteristics tend towards instabilities or filamentation. These problems can only be avoided with very narrow stripe widths ($\leqslant 3\ \mu$) [19], but in this case the above-mentioned ratio decreases to about 1.5. The development and the proper design of such lasers requires, therefore, an exact solution of the current spreading in the resistive layer. Such a solution is presented in this paper.

The mathematical treatment of the problem requires the simultaneous solution of the following two boundary value problems:

1) the diffusion equation for the carrier density in the active region,

2) Laplace's equation which governs the current flow in the resistive region.

These two partial differential equations are coupled to each other by the relationship of the injecting p-n junction. For the geometries we wish to consider here, Laplace's equation has to be solved in its two-dimensional form, while the diffusion equation can be reduced to one dimension. This simplification is made possible by the extremely small thickness of the active layer [20].

There are different techniques for the solution of Laplace's equation. First, one could use the finite element method which would provide a numerical solution. Second, it is possible to convert the boundary value problem into integral equations containing functions which are defined on the boundaries. As we are interested in potentials and current densities only at the boundaries, this technique becomes economical when used in actual numerical computation. We have actually used the

Manuscript received August 18, 1981; revised January 22, 1982. This work was supported in part by the Technological Program of the Federal Department of Research and Technology of the Federal Republic of Germany. The authors alone are responsible for the contents.

G. Lengyel was with the Research Laboratories, Siemens Corporation, Munich, Germany. He is now with the Department of Electrical Engineering, University of Rhode Island, Kingston, RI 02881.

P. Meissner and E. Patzak are with the Heinrich Hertz Institut für Nachrichtentechnik, Berlin, Germany.

K.-H. Zschauer is with the Research Laboratories, Siemens Corporation, Munich, Germany.

0018-9480/82/0400-0464$00.75

method of integral equations for the solution of this problem and obtained results very similar to the ones presented here. In this paper however, we use a third technique, that of conformal mapping, which is more applicable in this case and which is made possible by the relative simplicity of the geometry of the problem. This method provides an exact solution of the two-dimensional Laplace equation and is therefore superior to those mentioned above. The result expresses the current density distribution along the junction plane in terms of an arbitrary potential distribution along the same plane. It is valid for any stripe width to resistive layer thickness ratio. Any relationship between potential and carrier density at the p-n junction can be used, such as the customary Boltzmann approximation or the Fermi-Dirac formula as in [16]. The diffusion equation was solved numerically employing nonlinear spontaneous recombination terms applicable to bimolecular recombination. An iterative process led to a self-consistent solution to both problems. A short overview of this problem and its solution has already been given in [21].

II. Analysis

The geometry studied is shown in Fig. 1. The current supplied by the positively biased stripe contact has to pass through a resistive layer to reach the active region. The planes at $y = o$ and $y = -d$ are GaAs-GaAlAs heterojunctions, one of which is the injecting p-n interface. The resistive layer is usually p-doped, the active region can be either p- or n-doped. In the conventional laser structure, the resistive region consists most often of two layers: p-doped GaAlAs adjacent to the active region and p-doped GaAs near the metal contact. This practice which is used to improve the contact is not a necessity. We have fabricated lasers successfully contacting directly to the GaAlAs cladding layer. Therefore, in this paper the resistive layer was assumed to be homogeneous and was characterized by a single resistivity ρ. When the resistive region consists of two layers, this assumption is equivalent to neglecting the effects of the GaAs-GaAlAs p-p heterojunction, a reasonable assumption at the doping concentrations involved and taking the resistivities of the two layers to be equal. The spreading resistance in the substrate was neglected, as it is much lower than that of the resistive region and has little influence on the current distribution in stripe geometry lasers. Thus, the n-side of the p-n heterojunction was assumed to act as an equipotential sink. The carrier distribution in the active region which will finally determine the optical gain profile can be obtained by solving the diffusion equations for electrons and holes, respectively. Considering the fact that variations in the y-direction are extremely small in the very thin active region, integration of the continuity equations over the y-coordinate yields the following:

$$\frac{\partial n}{\partial t} = \frac{1}{e}\frac{\partial j_{xn}}{\partial x} - f(n) + \frac{j(x)}{ed}$$
$$\frac{\partial p}{\partial t} = -\frac{1}{e}\frac{\partial j_{xp}}{\partial x} - f(p) + \frac{j(x)}{ed}. \quad (1)$$

$n(x)$ and $p(x)$ represent the electron and hole concentrations in the active region, which in this case is assumed not to be doped. This does not represent any limitation of the technique, the method discussed below is equally applicable to doped active regions. f represents the recombination term and $j(x)$

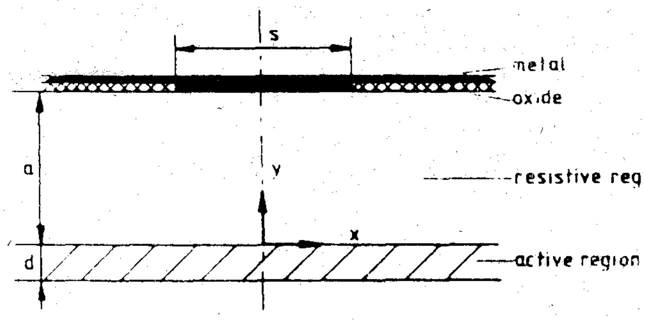

Fig. 1. Simplified geometry of the oxide-stripe laser diode.

the current density injected in the active region. j_{xn} and j_{xp} are the electron and hole current densities, respectively, which are directed in the x-direction. Considering the fact of charge neutrality and using terms for the current densities in the x-direction, one obtains the ambipolar diffusion equation for the steady state

$$D\frac{\partial^2 n}{\partial x^2} - f(n) + \frac{j(x)}{ed} = 0 \quad (2)$$

where D is the ambipolar diffusion coefficient. The diffusion coefficient may in general depend on the carrier distribution. We use the following recombination term in our calculations:

$$f(n) = Bn^2 + \frac{n}{\tau_D}$$

where B is the bimolecular recombination constant and τ_D is the spontaneous recombination lifetime.

The current density $j(x)$ ties the diffusion problem to the current flow problem of the resistive region which is governed by Laplace's equation

$$\frac{\partial^2 u}{\partial x^2} + \frac{\partial^2 u}{\partial y^2} = 0. \quad (3)$$

$u(x, y)$ is the potential inside or on the boundaries of the resistive region. The current density at any point in the resistive region is given by

$$\rho\vec{j} = -\nabla u. \quad (4)$$

Boundary conditions for (3) can be listed as

$$\text{at } y = a \text{ and } -s/2 < x < s/2, \qquad u = 0 \quad (5a)$$

$$\text{at } y = a \text{ and } -\infty < x < -s/2,\ s/2 < x < \infty, \qquad \frac{\partial u}{\partial y} = 0 \quad (5b)$$

$$\text{at } y = 0, \qquad u = U[n(x)]. \quad (5c)$$

The potential $U[n(x)]$ is equal to the voltage applied to the terminals of the diode minus the voltage drop across the p-n junction. The latter drop is given by

$$V = \frac{k_B T}{e}\left[\eta_1(n) + \eta_2(n) + \frac{E_g}{k_B T}\right]. \quad (5d)$$

$\eta_{1,2}$ are the quasi-Fermi levels measured from the valence and conduction bands, respectively, divided by $k_B T$.

The quasi-Fermi levels are functions of the carrier density. For the values of injected carrier density which are typical for the type of laser considered here, the quasi-Fermi levels are some k_BT inside the conduction band and about $\frac{1}{2}$ k_BT inside the valence band. For this reason, one has to take into account deviations from the Boltzmann distribution. Therefore we use an expression for the relation between the quasi-Fermi level η and the density, which was given in [22].

$$\eta_{1,2} = \left[\ln (n/N_{1,2}) + \sum_{i=1}^{4} \alpha_i (n/N_{1,2})^i\right]. \tag{6}$$

$N_{1,2}$ are the effective densities of states for the conduction band and the valence band, respectively. The formula was proved to be valid for our data.

Our task is to find the solutions of (2) and (3) with boundary conditions (5a)–(5d). As the two problems are so intimately linked to each other through the boundary conditions, one would have to find solutions simultaneously for both. For practical computations however, it seemed more advantageous to separate the two problems and first find solutions for only one of them. One can employ trial functions for some of the unknowns which appear in both problems and then check the correctness of these trial functions by solving the second problem. Comparison between result and trial function leads to an improved trial function with which the whole computation is repeated until a self-consistent solution to both problems is found.

A. Solution of the Two Dimensional Boundary Value Problem for the Current Density Distribution (Laplace Equation)

The solution was accomplished by the method of conformal mapping applicable to doubly connected regions [23]. It is assumed that the distribution of the potential $U(x)$ at the p–n junction is known and that the distribution of the current density at the junction has to be calculated. Since no current can flow through the oxide stripe, there is a line of flux directly along the junction between the resistive region and the oxide. Thus, the normal derivatives of the potential vanish there. This can be assured by reflection of the p–n junction at the oxide plane [Fig. 2(a)].

Since we have to deal with a doubly connected region, we have to solve this problem with the aid of the Schwarz-Christoffel transformation applicable to this case. By this transformation, the region is mapped into a period parallelogram, in which the potential problem can be solved easily. Fig. 2(a) gives the original and (b) gives the mapped configuration. Equivalent points are labeled with the same numbers. The mapping is chosen in such a way that the p-n junction is mapped on the lower line and the contact stripe on the upper side of the period parallelogram which because of the simple geometry becomes a rectangle. The choice of the points 2, 4, 6, 8 is taken for reasons of symmetry. The derivation of the transformation given in (7) is carried out in Appendix A.

$$w(z) = \frac{1}{4} + \frac{1}{2K(k^2)}\, tn^{-1}\left(e^{(\pi/2a)(s/2+z)}, k^2\right) \tag{7}$$

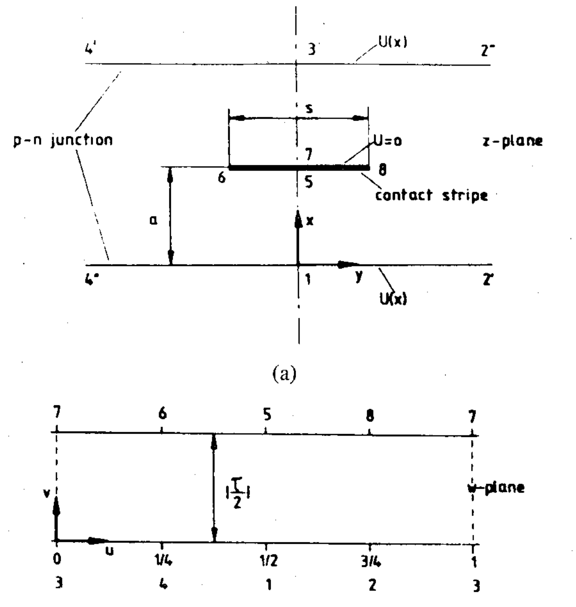

Fig. 2. Configuration of resistive layer (a) after reflection and (b) after mapping onto a period rectangle by the Schwarz-Christoffel transformation.

with

$$k^2 = 1 - e^{-\pi s/a} \quad \text{and} \quad \tau = i\,\frac{K'(k^2)}{K(k^2)}$$

where K is the complete elliptic integral of the first kind [24] for argument k, K' is the associate integral corresponding to K and $tn^{-1}(y, k)$ is the inverse of the Jacobian elliptic function [24].

We now have to solve the boundary value problem for the infinite long stripe of height $|\tau/2|$ and for periodic boundary values with periodicity one.

The complex potential for this problem can be written as

$$P(w) = C + Dw + \sum_n (A_n e^{i2\pi wn} + B_n e^{-i2\pi wn}). \tag{8}$$

The complex coefficients C, D, A_n, B_n have to be chosen in a way that the real part of $P(w)$ fulfills the boundary conditions. We leave out the explicit calculations and only give the result

$$P(w) = c_0\left(1 + 2i\frac{K}{K'}w\right) + \sum_{n=1}^{\infty} c_{2n}\left[\cos(4\pi nw) + \coth\left(2\pi n\frac{K}{K'}\right)\sin(4\pi nw)\right] \tag{9}$$

$$c_0 = 2\int_{1/2}^{3/4} U(u)\,du$$

$$c_{2n} = 4\int_{1/4}^{3/4} U(u)\cos(4\pi nu)\,du. \tag{10}$$

The current injected into the active region is proportional to the y-component of the electric field which we can get from (9)

$$j(x) = \frac{1}{\rho} E_y(x) = \frac{\pi}{4aK} \{[1 + e^{-(s\pi/2a)(1-2x/s)}] \cdot [1 + e^{-(s\pi/2a)(1+2x/a)}]\}^{1/2} \cdot \left\{ 2\frac{I}{l} + \frac{1}{\rho} \sum_{n=1}^{\infty} c_{2n} 4\pi n \coth\left(2\pi n \frac{K'}{K}\right) \cos\left(4\pi n\, u(x)\right) \right\}. \tag{11}$$

We have used the fact that the coefficient c_0 can be expressed with the total current I as

$$c_0 = \rho \frac{K'}{K} \frac{I}{l}. \tag{12}$$

Some aspects of the numerical evaluation of the series in (11) are discussed in Appendix B.

B. Solution of the Diffusion Equation

The diffusion equation is a nonlinear differential equation for which no analytic solution is available. We solved the equation numerically by a "shooting" method integrating the differential equation using an adaptive Romberg extrapolation. The initial value (dn/dx) at $x = 0$ is zero for reasons of symmetry. The value of $n(0) = n_0$ has to be found in such a way that $n(x)$ fulfills the boundary condition

$$\lim_{x \to \infty} [n(x)] \to 0.$$

This completes the solution of the two boundary value problems which describe the operating conditions of the laser below or slightly above threshold when stimulated recombination is not yet significant. Stimulated recombination can be included in this model by adding a stimulated recombination term to the diffusion equation (2). This term requires the knowledge of the photon-field distribution which in turn can be obtained from the solution of the EM wave equation, for which this model supplies accurate gain profiles. Such complete calculations have already been carried out successfully using this model.

III. Results and Discussions

The influence of several geometrical and physical parameters on the solutions was studied in detail. In this respect, the magnitude and shape of the various distributions (current- and carrier-densities) deserve attention. The basic set of parameters used in the calculation are summarized in Table I. Material constants such as D, B, and τ_D were taken from measurements and these values seem to describe well the transient behavior of our lasers.

Fig. 3 shows, for the parameters of Table I, the distribution of the carrier density in the active region n, the current density at the p-n junction j, and the current density at the stripe

TABLE I

$\rho = 0.2\ \Omega \cdot \text{cm}$	$D = 40\ \text{cm}^2/\text{s}$
$s = 3\ \mu\text{m}$	$B = 9.7 \times 10^{-11}\ \text{cm}^3/\text{s}$
$a = 2\ \mu\text{m}$	$\tau_D = 1.8 \times 10^{-8}\ \text{s}$
$d = 0.1\ \mu\text{m}$	$T = 300\ \text{K}$
$I = 100\ \text{mA}$	

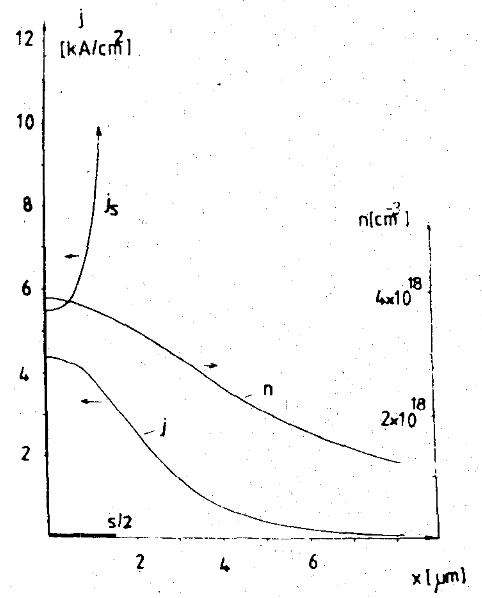

Fig. 3. Current- and carrier-density distributions for data of Table I. j: current density injected into active region; j_s: current density along stripe contact.

contact j_s. A characteristic feature of this and all other solutions supplied by this model is the singularity in j_s at $\pm s/2$ which has not been pointed out by previous authors and may have practical consequences for contact fabrication. Furthermore, the variation of the current density j along the p-n junction is smooth and free from discontinuities in its higher derivatives at $\pm s/2$ which appear in many solutions where the region is arbitrarily divided into two parts: one below the contact stripe and one outside it.

Fig. 4 shows the effect of stripe width on the current density along the p-n junction. At larger stripe width, the distribution has a local minimum in the center which has not been recognized by previous authors and which is caused by the nonlinear boundary condition introduced by the p-n junction. This local minimum appears at narrower stripe widths as well but only at lower resistivities.

Fig. 5 shows the effect of the thickness of the resistive layer on the current density along the p-n junction. The form of these distributions depends principally on the s/a ratio [see (11)] as long as the influence of the potential distribution along the junction is negligible, that is when the specific resistivity is relatively high.

A central problem in the design of oxide-stripe lasers is the assurance of firm lateral guidance of the EM wave which is provided by the gain profile. The curvature at the center

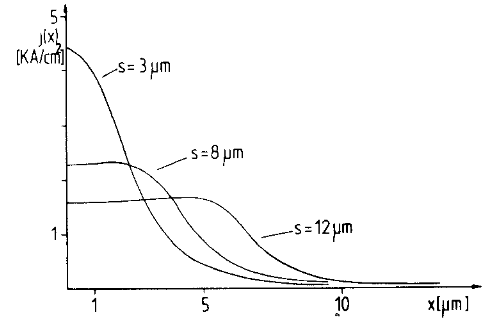

Fig. 4. Current density distributions injected into active region as a function of stripe width. All other parameters are as in Table I.

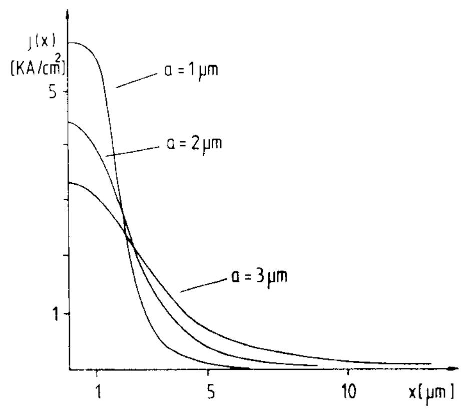

Fig. 5. Current density distributions injected into the active region as a function of the thickness of the resistive layer. All other parameters are as in Table I.

$d^2g/dx^2|_{x=0}$ is a measure of how well the laser resists the flattening of this profile at higher outputs when spatial hole burning depletes the carriers in the center [16]. When this curvature becomes zero or negative, guidance ceases and kinks or instabilities appear in the light-current characteristics. The requirement $d^2g/dx^2|_{x=0} > 0$ also means in first approximation that $d^2n/dx^2|_{x=0} > 0$.

Fig. 6 shows the variation of $d^2n/dx^2|_{x=0} = n''(0)$ as a function of stripe width. The decrease is practically exponential indicating that narrow stripe widths significantly improve the lateral guidance.

The effect of the specific resistivity ρ is shown in Fig. 7. All three curves begin to saturate above $\rho > 0.3\ \Omega \cdot \mathrm{cm}$. Above this value, the effect of the p-n junction on the solution of the potential problem becomes negligible, and the solution of the two problems can be separated from each other. The exact solution of the potential problem is then given by the simpler first part of (11) as the second, containing the potential, vanishes as $\rho \to \infty$. This $j(x)$ serves then as the driving function of the diffusion problem. Below $\rho \sim 0.3\ \Omega \cdot \mathrm{cm}$, all three curves decrease rapidly. The decrease of $n''(0)$ points to a dilemma because of the above-mentioned reasons of stability. Low resistivities are desirable nevertheless to reduce ohmic losses and improve temperature and aging characteristics. The compromise between the conflicting requirements of low thermal losses and good lateral guidance must necessarily lead to narrow stripe widths. The validity of these considerations was proven by the fact that it was possible, using these principles, to develop narrow-oxide-stripe lasers with outstanding temperature stability (up to 120 °C) extremely low aging ($10^{-5}\ h^{-1}$ at 100 °C) and smooth, kink-free characteristics up to over 100 mW/facet in pulsed operation [25]. The effect of the variation of other parameters was also studied, but the results were less interesting and do not warrant detailed discussion. One might mention that the variation of the ambipolar diffusion constant D results only in minor changes, indicating that the assumption of a constant D is justified, although strictly speaking, ambipolar diffusion can only be described by density-dependent diffusion constants.

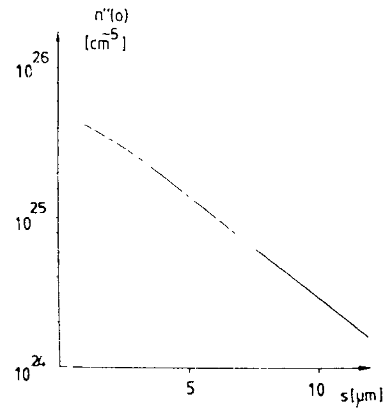

Fig. 6. Curvature of carrier density distribution at the center as a function of stripe width. Other parameters are as in Table I.

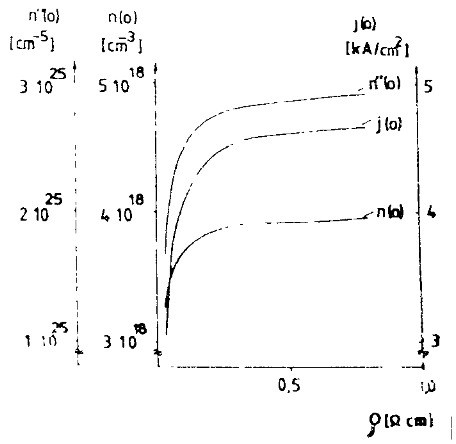

Fig. 7. Effect of the specific resistivity on some laser parameters. Other data are as in Table I.

The effect of B and τ_D on the results, within a region of reasonable values, was found negligible. The same applies to the temperature dependence of the voltage across the p-n junction.

IV. Summary and Conclusions

Analysis of lateral guidance in stripe geometry DH lasers requires the knowledge of the lateral distribution of the complex refractive index which is proportional in first order to the charge carrier density present in the active region. A complete solution of this problem requires knowledge of the carrier density distribution which can be obtained by the simultaneous solution of two boundary value problems: the diffusion equation for the carriers in the active region and Laplace's equation for the current distribution in the resistive layer. These two boundary value problems are coupled by a nonlinear relation at one of the boundaries. In this work, an exact solution of the two-dimensional Laplace equation is given. The result expresses the current density distribution along the junction plane in terms of an arbitrary potential distribution along the same plane. The mathematical technique is applicable to any stripe width to resistive layer thickness ratio. Any relationship between potential and carrier density at the p-n junction can be used, such as the customary Boltzmann approximation or the more accurate Fermi-Dirac formula. The diffusion equation was solved numerically employing nonlinear spontaneous recombination terms applicable to bimolecular recombination. An iterative process led to a self consistent solution to both problems.

One of the results of the calculation was the recognition that the current density supplied by the stripe contact has an integrable singularity at the two edges of the stripe. Furthermore, local minima may appear in the center of the current density distribution injected into the active region particularly at low resistivities and wide stripe widths.

The calculations point towards the need of finding a suitable compromise in choosing the specific resistivity of the resistive region. On the one hand, one would require low resistivities in order to reduce ohmic losses and temperature rise. Resistance to spatial hole burning and ensuring kink-free characteristics, on the other hand, call for higher specific resistivities. A satisfactory compromise can only be found when very narrow stripe widths are chosen.

In sheet-resistance models, which are used widely according to the published literature, the behavior of the current density distribution is characterized, among other things, by the sheet resistance ρ/a. Our solutions show otherwise; ρ, a and other geometrical factors influence the solutions independently. The results further indicate that the usual assumptions about the current distribution and the one-dimensional treatment of the resistive layer are not always justified, particularly for low values of ρ and s. This region of ρ and s values, however, is exactly the one of great practical interest if one wishes to design oxide-stripe lasers having high temperature stability and kink-free light-current characteristics. For larger values of the resistivity ($\rho > 0.3$ cm) the solution of the potential and diffusion problems can be separated from each other. The current density distribution along the injecting interface can then be approximated by a relatively simple expression, which is also the exact solution of the potential problem for $\rho \to \infty$.

Appendix A

The transformation mapping the configuration of Fig. 2(a) into the periodic rectangle of Fig. 2(b) is

$$z(w) = C_1 \int \prod_{\mu=1}^{m} [\vartheta_1(w - d_\mu, \tau)^{(\alpha_\mu - 1)/\pi}]^{-1} \cdot \prod_{\nu=1}^{n} [\vartheta_4(w - e_\nu, \tau)^{(\beta_\nu - 1)/\pi}]^{-1} \, dw + C_2. \tag{A1}$$

TABLE II
THE CONSTANTS OF THE CONFORM MAPPING

μ	1	2	3	4
z_μ	0	∞ ∞+2ja	2ja	-∞+2ja -∞
d_μ	1/2	3/4	1 0	1/4
α_μ	π	0	π	0

	5	6	7	8
z_ν	ja	-s/2+ja	ja	-s/2-ja
e_ν	1/2	1/4	1 0	3/4
β_ν	π	2τ	π	2π

$\vartheta_{1,4}$ is the $\vartheta_{1,4}$ function of Weierstraß, n is the number of points on the lower line and m is the number of points on the upper line of the periodic rectangle. The angles α_ν and β_ν are the interior angles of the original configuration, the constants d_μ, e_ν are the x-coordinates in the w plane and C_1, C_2 are complex constants. The values of the constants are given in Table II.

The resulting transformation is

$$z(w) = C_1 \int_0^w \vartheta_1^{-1}(w - \tfrac{1}{4}, \tau)\, \vartheta_1^{-1}(w - \tfrac{3}{4}, \tau) \cdot \vartheta_4(w - \tfrac{1}{4}, \tau)\, \vartheta_4(w - \tfrac{3}{4}, \tau)\, dw + C_2. \tag{A2}$$

The following equations determine the unknown constants C_1, C_2, τ [19]:

$$z(w) = z(w + 1) \tag{A3}$$

$$z(w + \tau) = z(w) + 2ja \tag{A4}$$

$$z(0) = 2ja \tag{A5}$$

$$z(\tau/2 + \tfrac{3}{4}) = ja + s/2. \tag{A6}$$

We have eight real equations for five real parameters. There are more equations than unknown constants because of the assumption of symmetry. Since the integrand is a double periodic function, it can be expanded in the ζ function of Weierstraß [24]

$$z(w) = B \int [\zeta(w + \tfrac{1}{4}, \tau) - \zeta(\tau/2 + \tfrac{1}{2}, \tau) - \zeta(w - \tfrac{1}{4}, \tau) + \zeta(\tau/2, \tau)]\, dw + C_2.$$

The integral yields

$$z(w) = -B \ln \frac{\vartheta_1(w - \frac{1}{4}, \tau)}{\vartheta_1(w + \frac{1}{4}, \tau)} + D. \tag{A7}$$

The unknown constants such as B, D, and τ can be determined using the equations (A3)-(A6). The result is

$$z(w) = s/2 + \frac{2a}{\pi} \ln\, [tn(2K(k^2)(w - \tfrac{1}{4}), k^2)]$$

with

$$k^2 = 1 - e^{-\pi s/a}.$$

Appendix B

The numerical evaluation of (11) presented some problems as the series in the second term converges only slowly. A way out of this difficulty is the splitting of the series

$$\sum_{n=1}^{\infty} C_{2n} 4\pi n \coth\left(2\pi n \frac{K'}{K}\right)\cos(4\pi n u(x)) \tag{B1}$$

into the following two parts:

$$\sum_{n=1}^{\infty} C_{2n} 4\pi n \left[\coth\left(2\pi n \frac{K'}{K}\right) - 1\right]\cos(4\pi n u(x)) \tag{B2}$$

$$+ \sum_{n=1}^{\infty} C_{2n} 4\pi n \cos(4\pi n u(x)). \tag{B3}$$

$\coth(4\pi n K'/K) - 1$ is rapidly decreasing with n and we only have to calculate a few coefficients c_{2n} for this part of the series. The second part can be converted into a more suitable form. We notice that

$$\sum_{n=1}^{\infty} c_{2n} 4\pi n \cos(4\pi n u(x))$$

is the imaginary part of

$$\sum_{n=1}^{\infty} c_{2n} 4\pi n i e^{i4\pi n u(x)} = F(u). \tag{B4}$$

The real part of $F(u)$ is the derivate of the potential at the active layer (apart from a factor du/dx). Because $F(u)$ is analytic in the upper half-plane we can calculate the imaginary part from the known real part with the aid of the Hilbert transformation.

Glossary of Symbols

a:	thickness of the resistive region,
B:	quadratic recombination constant,
D:	ambipolar diffusion constant,
e:	elementary charge,
E_g:	bandgap,
$f(n)$:	recombination term,
i:	imaginary unit,
I:	current,
j:	current density,
j_{xn}:	x-component of the electron current density,
j_{xp}:	x-component of the hole current density,
k:	modulus of elliptic integral,
k_B:	Boltzmann's constant,
$K(k)$:	complete elliptic integral of the first kind,
$K'(k)$:	associated complete elliptic integral of the first kind,
l:	length of the laser,
n:	electron density,
$N_{1,2}$:	effective densities of state for electrons and holes, respectively,
p:	hole density,
$P(w)$:	complex potential,
s:	stripe width,
$tn^{-1}(y, k)$:	inverse of the Jacobian elliptic function,
T:	temperature,
$u(x, y)$:	potential,
$U(n(x))$:	potential at the active region-resistive region interface,
V:	voltage drop across the active region,
α_μ:	interior angles in the z-plane,
β_μ:	interior angles in the z-plane,
ζ:	ζ function of Weierstraß,
$\eta_{1,2}$:	quasi-Fermi levels for electrons and holes,
$\vartheta_{1,4}$:	$\vartheta_{1,4}$ functions of Weierstraß,
ρ:	specific resistance,
τ:	width of the period rectangle,
τ_D:	spontaneous recombination lifetime.

References

[1] I. Hayashi, M. B. Panish, P. W. Fry, and S. Sumski, "Junction lasers which work continuously at room temperature," *Appl. Phys. Lett.*, vol. 17, pp. 105–111, 1970.
[2] H. Kressel and H. Nelson, "Close confinement GaAs p-n junction lasers with reduced optical loss at room temperature," *RCA Rev.*, vol. 30, pp. 106–113, 1969.
[3] Z. I. Alferov, V. M. Andreev, E. L. Portnoi, and M. K. Trukan, "AlAs-GaAs heterojunction injection laser with a low room temperature threshold," *Sov. Phys. Semicond.*, vol. 3, pp. 1107–1110, 1970.
[4] D. D. Cook and F. R. Nash, "Gain-induced guiding and astigmatic output beam of GaAs lasers," *J. Appl. Phys.*, vol. 46, pp. 1660–1672, 1975.
[5] T. L. Paoli, "Wave guiding in a stripe-geometry junction laser," *IEEE J. Quantum Electron.*, vol. QE-13, pp. 662–668, 1977.
[6] W. B. Joyce and S. H. Wemple, "Steady-state junction-current distributions in thin resistive films on semiconductor junctions (solutions of $\nabla^2 V = \pm e^{-V}$)," *J. Appl. Phys.*, vol. 41, pp. 3818–3830, 1970.
[7] W. P. Dumke, "Current thresholds in stripe-contact injection lasers," *Solid State Electron.*, vol. 16, pp. 1279–1298, 1973.
[8] B. W. Hakki, "Carrier and gain spatial profiles in GaAs stripe geometry lasers," *J. Appl. Phys.*, vol. 44, pp. 5021–5028, 1973.
[9] ——, "GaAs double heterostructure lasing behaviour along the junction plane," *J. Appl. Phys.*, vol. 46, pp. 292–302, 1975.
[10] H. S. Sommers, "Experimental properties of injection lasers: Modal distribution of laser power," *J. Appl. Phys.*, vol. 44, pp. 1263–1275, 1973.
[11] I. Ladany, "The influence of stripe width on the threshold current of double-heterostructure lasers," *J. Appl. Phys.*, vol. 49, pp. 1935–1950, 1977.
[12] P. Kirkby, A. R. Goodwin, G.H.B. Thompson, and P. R. Selway, "Observation of self-focusing in stripe geometry semiconductor lasers and the development of a comprehensive model of their operation," *IEEE J. Quantum Electron.*, vol. QE-13, pp. 709–719, 1977.
[13] N. Chinone, "Nonlinearity in power-output-current characteristics of stripe-geometry injection lasers," *J. Appl. Phys.*, vol. 48, pp. 3237–3243, 1977.
[14] W. T. Tsang, "The effects of lateral current spreading, carrier outdiffusion, and optical mode losses on the threshold current density of GaAs-$Al_xGa_{1-x}As$ stripe-geometry DH lasers," *J. Appl. Phys.*, vol. 49, pp. 1031–1044, 1978.
[15] H. Yonezu, I. Sakuma, K. Kobayashi, T. Kamejima, M. Ueno, and Y. Nannichi, "A GaAs/$Al_xGa_{1-x}As$ double heterostructure planar laser," *Japan J. Appl. Phys.*, vol. 12, pp. 1585–1592, 1973.
[16] W. B. Joyce, "Current crowding and carrier confinement in double heterostructure lasers," *J. Appl. Phys.*, vol. 51, pp. 2394–2401, 1980.
[17] G.H.B. Thompson, *Physics of Semiconductor Laser Devices*. New York: Wiley, 1980, pp. 315–319.

[18] S. Wang, C. Y. Chen, A. S. Liao, and L. Figueroa, "Control of mode behavior of semiconductor lasers," *IEEE J. Quantum Electron.*, vol. QE-17, pp. 453-468, Apr. 1981.
[19] R. Lang, "Lateral transverse mode instability and its stabilization in stripe geometry injection lasers," *IEEE J. Quantum Electron.*, vol. QE-15, pp. 718-726, 1979.
[20] B. W. Hakki, "Mode gain and junction current in GaAs under lasing conditions," *J. Appl. Phys.*, vol. 45, pp. 288-294, 1974.
[21] G. Lengyel, P. Meissner, E. Patzak, and K.-H. Zschauer, "Calculation of lateral current spreading and series resistance effects in oxide stripe geometry DH GaAs-GaAlAs lasers," *Electron. Lett.*, vol. 17, pp. 174-175, 1981.
[22] W. B. Joyce and R. W. Dixon, "Analytic approximations for the Fermi energy of an ideal Fermigas," *Appl. Phys. Lett.*, vol. 31, pp. 354-356, 1977.
[23] W. von Koppelfels and F. Stallmann, *Praxis der Konformen Abbildung*. Berlin: Springer, 1959, pp. 344-347.
[24] P. F. Byrd and M. O. Friedman, *Handbook of Elliptic Integrals for Engineers and Scientists*. Berlin: Springer, 1971.
[25] H. D. Wolf, K. Mettler, and K.-H. Zschauer, "High performance 880 nm (GaAl)As/GaAs oxide stripe lasers with very low degradation rates at temperatures up to 120°C," *Japan J. Appl. Phys.*, vol. 20, pp. 693-696, 1981.

G. Lengyel (M'59) received the B.S. degree from the Technical University of Budapest, Budapest, Hungary, in 1950 and the Ph.D. degree from the University of Toronto, Toronto, Ont., Canada, in 1964, both in electrical engineering.

Currently, he is a Professor of Electrical Engineering at the University of Rhode Island, Kingston. Since 1972 he has been a Guest Scientist at the Research Laboratories, Siemens Corporation, Munich, Germany, where he has worked on various research projects connected with the development of GaAlAs/GaAs DH lasers.

Dr. Lengyel is a member of the American Physical Society and the American Optical Society.

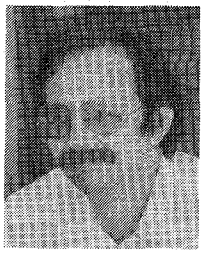

Peter Meissner was born in Adelsdorf, Germany, on November 28, 1943. He received the Dipl. Ing. degree in 1971 and the Dr. Ing. degree in 1977, both in electrical engineering, from the Technical University, Berlin, Germany.

Since 1971 he was with the Heinrich Hertz Institut für Nachrichtentechnik, Berlin, Germany, where he was engaged in research on navigation systems. Presently, he is working on the theory of semiconductor injection lasers.

Erwin Patzak was born in Minstedt, Germany, on July 27, 1949. He received the Diplom degree in physics in 1974 and the Dr.rer.nat. degree in 1980 from the Universität Hannover, Hannover, Germany.

From 1974 to 1980 he worked on the theory of solid-state magnetism at the Institut für Theoretische Physik, Universität Hannover, Hannover, Germany. In 1980 he joined the Heinrich Hertz Institut für Nachrichtentechnik, Berlin, Germany, where he is currently working on the theory of the semiconductor laser.

K.-H. Zschauer, photograph and biography not available at the time of publication.